Journal of Materials Chemistry A

Accepted Manuscript

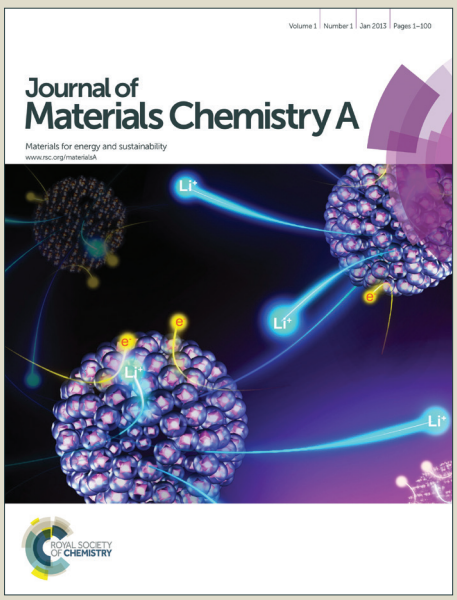

ROYAL SOCIETY OF CHEMISTRY

www.rsc.org/materialsA

Journal of Materials Chemistry A RSCPublishing

ARTICLE

High pressure treated ZnO ceramics towards giant dielectric constant

Cite this: DOI: 10.1039/x0xx00000x

Xuhai Li, Liang Xu, Lixin Liu, Yuan Wang, Xiuxia Cao, Yuanjie Huang, Chuanmin Meng*, and Zhigang Wang*

Received 00th January 2014,
Accepted 00th January 2014

DOI: 10.1039/x0xx00000x

www.rsc.org/

ZnO ceramics with giant dielectric constant have been synthesized *via* a high pressure treating method. SEM results reveal that the ceramics using high pressure treated powders are porous, and the dielectric constant of specimens first increases and then decreases with increasing density. Ceramics sintered at 1050 °C possess the optimal giant room temperature dielectric constants (~1.8×10^4 at 100 Hz) with low relative density and dielectric loss. The improved dielectric constant can be attributed to enhanced Maxwell-Wagner poly-dispersive relaxation due to the high pressure treating process, which makes ZnO porous ceramics a potential material for high dielectric constant applications. This approach is generic and provides a new avenue to obtain porous ceramics with excellent dielectric properties.

1. Introduction

The miniaturization of modern microelectronic devices and high-energy density storage applications have aroused tremendous attention to giant dielectric constants ($\varepsilon > 10^3$) materials, which are attributed to their ability to reduce the size of capacitive components.[1] Most of the currently available capacitor materials with giant dielectric constants are ferroelectrics, such as $BaTiO_3$. Unfortunately, the strong temperature dependence of ε limits their applications.[2] Nowadays several non-ferroelectric transition-metal oxides including $Ca[(Li_{1/3}Nb_{2/3})_{1-x}Ti_x]O_{3-\delta}$-Ag (CLNTA),[3] $(In_{0.5}Nb_{0.5})_xTiO_2$ (INTO),[4] $Li_xTi_yNi_{1-x-y}O$ (LTNO),[5] $CaCu_3Ti_4O_{12}$ (CCTO),[6] $Ni_{0.5}Zn_{0.5}Fe_2O_4$,[7] and $LaFeO_3$ are found to exhibit giant ε values on an order of magnitude of 10^4 and stable ε during the temperature change.[8] Among them, the giant ε values of CLNTA, INTO and LTNO are derived from the doping effect by forming percolation, electron-pinned defect-dipole, or unique microstructure. While the giant dielectric response of others (*i.e.* CCTO) can be attributed to Maxwell-Wagner polarization resulting from inhomogeneous electrical properties between grains and grain boundaries, contact effect between the metallic electrodes and the bulk sample, and intrinsic polaron-type origin due to localized carriers hopping between ions with mixed-valence states.[6-9] Despite huge efforts, the aforementioned materials do not seem ideal for straightforward application especially considering the difficulty of preparing pure phase and the amplitude of the dielectric loss.[5-8] Further improvement are still needed to be done before these materials systems are viable for commercial applications in devices. Thus there is still an ongoing search for new, better giant dielectric constant materials.

Comparing to the multi-component high dielectric constant materials, such as CCTO, ZnO is easier to prepare in the pure form and available commercially in large scale with low cost. In the past decade, zinc oxide (ZnO) has attracted much attention due to its wide direct band gap (E_g~ 3.3 eV) and large exciton binding energy (60 meV),[10] which can provide an impact on applications in piezotronics,[10] varistors,[11] super-capacitors,[12] and thermoelectric devices.[13] Despite the dielectric behaviours of various types of ZnO nano-structures,[14] films,[15] and ceramics have been conducted at a wide range of temperatures and frequencies,[11a,16] the relative dielectric constant of pure ZnO is still quite low (< 1500 at 100 Hz). Recently, Tripathi *et al.* found ZnO nano-structure synthesized by soft chemical method exhibits a high dielectric constant of 10^4 at low frequency, making it a candidate material for capacitor applications, but the nano-ZnO bulks were not sintered body, and the dielectric constants decrease rapidly with increasing frequency.[14a]

The dielectric constants of ceramics are greatly influenced by the porosity (its mount and geometrical morphology).[17a,b] Controlled porosity could produce giant permittivity in porous ceramics, e.g. high dielectric constants of the order of 10^6 have been found in porous alumina ceramics due to the geometrical and interfacial effects.[17c] The porous ceramics are usually obtained by combine ceramic powders with porosity formers (like passive polymers, carbon black, starches) and sintering at high temperature.[17] Nevertheless, these processes are non-environment friendly, and the residual matters of these additives are detrimental to the relative permittivity of ceramics.[17b] Herein, we report a new, simple, and environment-friendly method to prepare porous ZnO ceramics by conventional sintering high pressure treated ZnO nano powders without any additives. These novel porous ZnO ceramics display giant dielectric permittivity with stable frequency and temperature independence. The impedance and dielectric analysis results show high pressure treating process plays a critical role in enhanced dielectric performance of ZnO, which is attributed to the porous, low-density, especially, low grain boundary resistance.

2. Experimental

High purity commercially available ZnO (99.9%, Aladdin) nano powder with grain size distributing in the range of 37 ~ 452 nm (average ~ 125 nm) was used to fabricate the ZnO ceramics. Firstly, the powder was loaded into a mould and shaped using a cold press method. The as-prepared bulk was inserted into a Mo crucible and loaded into a high pressure apparatus for high pressure treating (HPT). The HPT was carried out under 4.4 GPa for 5 min on a multi-anvil apparatus (YT-800, Guilin Zhuye Corp. China) at room temperature. Then the product was ground into powder, pressed into discs of about 8 mm in diameter using a cold press method. The as-prepared discs were sintered at 900-1300 °C for 2 h in a conventional electric furnace and then cooled down to room temperature in air. For comparison, ZnO ceramics without HPT were sintered at 1050 °C for 2 h (designed as CS-1050 °C). Finally, both sides of the obtained products were polished and cleaned.

The bulk density was obtained using the Archimedes method. The crystalline phase identification was determined using X-ray diffractometry (X'pert Pro, PANalytical, the Netherlands) with Cu Kα radiation. The microstructures of the ZnO ceramic pieces were characterized by scanning electron microscopy (SEM, FEI Quanta 250, USA). After coating with silver paste on both sides of the ZnO pieces, the electrode contacts were cured at 100 °C for 3 h. Finally, after aging for 24 h, the dielectric response and AC impedance spectra of the specimens were measured using an Agilent 4294A Precision LCR Meter (Agilent Technologies Inc. USA) over a frequency range of 40-100 MHz.

3. Results and discussion

Porous ZnO ceramics are prepared *via* conventional ceramic processing HPT precursor. To demonstrate the merit of HPT, ZnO ceramics are also prepared using the precursor of ZnO powder without HPT. The XRD patterns of prepared ZnO specimens are shown in Figure S1. The peaks in the figure are indexed to the hexagonal wurtzite structure of ZnO (No. 36-1451 JCPDS card). No evidence of any other phases is presented in the patterns.

Figure 1(a)-1(h) show the fracture surface SEM images of ZnO specimens sintered at 950 °C, 1050 °C, 1150°C and 1250 °C using HPT precursor, respectively, and Figure 1(i) and 1(j) shows the fracture SEM images of 1050 °C sintered specimen using the precursor of ZnO powder without HPT. It is obvious that all the ceramics prepared with HPT precursor present porous microstructures with relative density 84~89%, while ceramic sintered at 1050 °C without HPT presents a more dense structure (with a high relative density of ~97%). These results indicating that conventional sintering HPT precursor is an effective way to produce porous structure in ZnO ceramics without any additives. The porous structures are mainly caused by the inhomogeneous sintering ability of ZnO HPT precursors. Figure S2(a) shows the microstructure of ZnO precursor after HPT process. It is obvious that the treatment at 4.4 GPa compacts the powders to a well dense bulks, while the following grinding process broken up them into small particles which are composed with dense nano grains as shown in Figure S2(b). This leads the as pressed discs using these HPT precursors exhibit large amounts of voids because the ZnO particles are more difficult to compact than powders. The inner parts of ZnO particles are easy to form dense structure, while the voids between ZnO particles are difficult to eliminate during sintering, and thus form porous structure.

Figure 2 shows the relative density and grain size of ZnO ceramics as a function of sintering temperature. It is determined that an increase to the sintering temperature corresponded to an increase in both relative density and grain size. For the specimen sintered at 950 °C, the density and grain size is as low as 4.78 g cm^{-3} (~84% of theory density) and 480 nm respectively. As the sintering temperature increases to 1050 °C, the density and grain size increases to ~ 4.81 g cm^{-3}, ~1.24 μm. When the sintering temperature is further increased to 1150 °C, the density increases to ~4.83 g cm^{-3} (~85% of theory density), and the grain size increases to ~1.85 μm. For the 1250 °C sintered specimen, the density is ~5.03 g cm^{-3} (~89% of theory density), and the average grain size is ~2.85 μm. In sharp contrast, the density of ceramics sintered at 1050 °C without HPT is ~5.51 g cm^{-3} with grain size of ~2.27 μm, significantly higher than the ZnO ceramics sintered at 1050 °C with HPT. The results indicate that the HPT process can suppress the recrystallization of ZnO powders and leads to the formation of porous ZnO ceramics and reduce the density of ceramics.

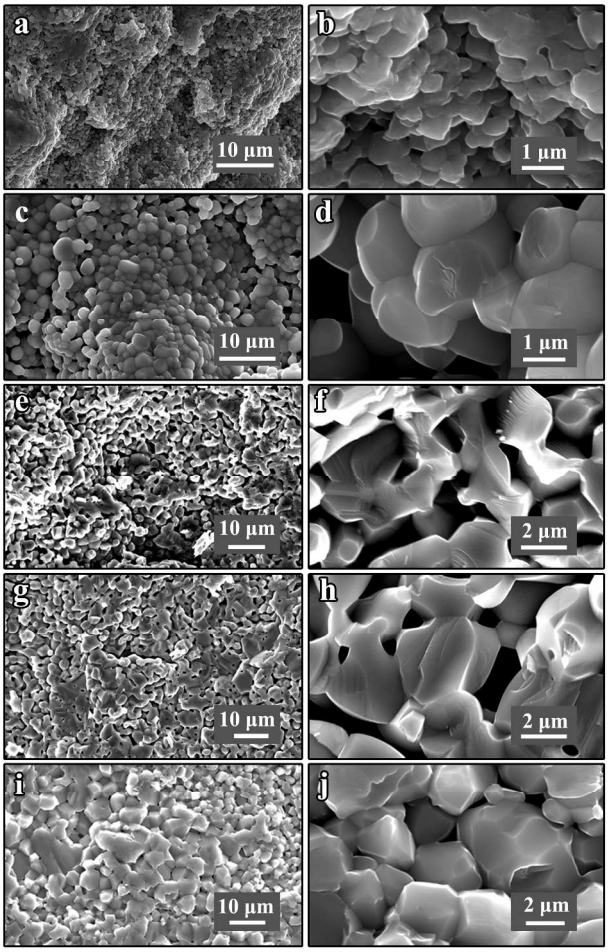

Figure 1 SEM images of fractured surface of ZnO ceramics sintered at (a), (b) 950°C, (c), (d) 1050°C, (e), (f) 1150 °C, (g), (h) 1250 °C with HPT, and (i), (j) 1050 °C without HPT.

The ac impedance spectra of the ZnO ceramics sintered at 950-1250 °C with and without HPT on a Nyquist plot (Z''vs Z') was interpreted using an equivalent circuit model as shown in Figure 3. The depressed semi-circles suggesting the appearance of non-Debye type relaxation due to the heterogeneity of the barriers of the specimens.[11b] All the samples with HPT show two overlapping semi-circles which can be modeled by a

parallel RC equivalent circuit, where R represents the resistance and C is the geometric capacitance of the specimens.[16] The large semi-circles on the right side at the low frequency parts were the grain boundary arcs, while the small ones on the left side at the high frequency parts correspond to the grain interior arcs.[19] Nevertheless, specimen sintered at 1050 °C without HPT presents just one semi-circle while with large diameter, corresponding to a large grain boundary resistance (R_{gb}) owing to its high density. It is apparent that the resistance of grain boundaries is much larger than that of grain interior (R_g) at room temperature, which indicates that grain boundaries are important for electrical resistivity.[9] Consequently, the value of dielectric constant ε' can be calculated by: [11b]

$$\varepsilon' = \frac{d}{2\pi A \varepsilon_0 f_p R_{gb}} \quad (1)$$

where ε_0 is the vacuum permittivity, A and d is the electrode area and thickness of the samples, f_p is the relaxation frequency.

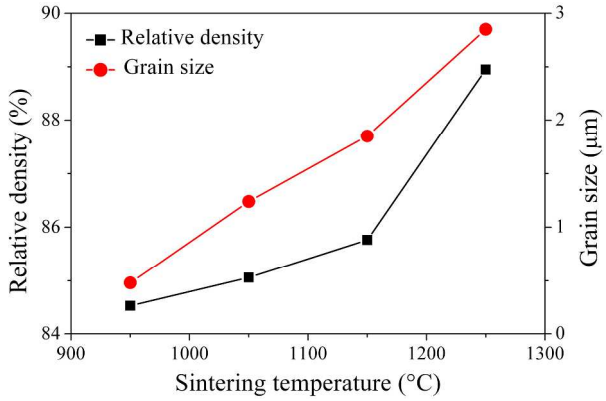

Figure 2 Relative densities and grain size of high pressure treated ZnO ceramics as a function of sintering temperature.

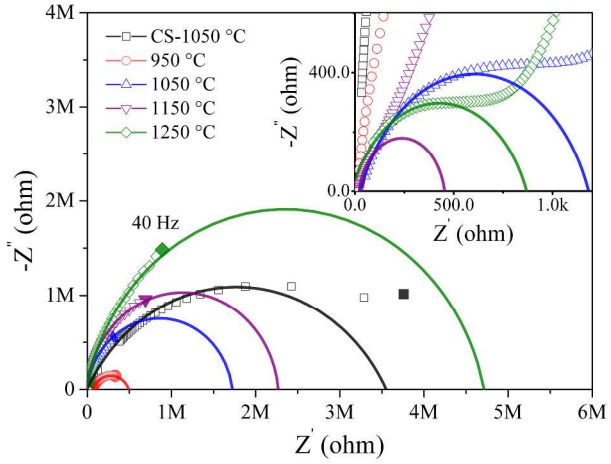

Figure 3 Nyquist plots of the ZnO samples measured at room temperature, the inset is the enlarged spectra. The solid dots are impedances at 40 Hz.

Table 1 shows the variation of R_g and R_{gb} with sintering temperature for the ceramics with and without HPT. It is obvious that R_g decreases, while R_{gb} increases with increasing sintering temperature due to the improved density, as shown in Figure S3. The relaxation frequency f_p (where the imaginary impedance Z'' reach its maximum) decreases with increasing sintering temperature due to the improved resistance, yielding f_p ~67 Hz for 950 °C sintered specimen, below 40 Hz for ceramics sintered at higher temperature, and ~488 Hz for the sample without HPT, as shown in Figure 3. Thus, specimen with HPT sintered at 1050 °C may exhibit excellent dielectric properties due to its lower f_p and R_{gb}. It has been clearly demonstrated the relaxation phenomenon is related to the space-charge polarization (Maxwell-Wagner polarization) since the relaxation frequency f_p is lower than 10 Hz.[11b] Therefore, space-charge polarization is significant for the high pressure treated ceramics to enhance the dielectric performance with HPT.

Table 1 Variation of R_g, R_{gb} and f_p with sintering temperature (T_s) for ZnO ceramics with and without HPT.

T_s (°C)	R_g (Ω)	R_{gb} (Ω)	f_p (Hz)
950	8.81×10^4	5.05×10^5	67
1050	1180	1.74×10^6	< 40
1150	451	2.28×10^6	< 40
1250	867	4.73×10^6	< 40
CS-1050	4128	3.56×10^6	488

Figure 4(a) and 4(b) show the relation of relative dielectric constant (ε') and dielectric loss ($\tan\delta$) with frequency at room temperature for ZnO ceramics. As shown in Figure 4(a), ε' of the sample without HPT is very low, and decreases rapidly with increasing frequency which is in compliance with the universal dielectric response of dielectrics;[19b] interestingly, ceramics using HPT ZnO precursor present giant ε' at low frequency ranges which are much higher than that of ceramics without HPT. ε' for specimen sintered at 950 °C decreases sharply with increasing frequency due to its low grain boundary resistance, while for specimens sintered at higher temperature, ε' decrease slightly at frequency around 100 kHz then decreases sharply with further increase of frequency. And $\tan\delta$ of all specimens with HPT possess a broad relaxation peak at high frequency, corresponding to the character of Debye-like relaxation.[19] In addition, the position of loss peak ($\tan\delta_m$) shifts to higher frequency with increasing sintering temperature due to the formation of an effective depletion layer at the grain boundaries.[11b]

The relaxation of ε' and $\tan\delta$ can be explained by ideal Debye relaxation and Maxwell-Wagner relaxation model.[8,19,20] The difference between Debye relaxation and Maxwell-Wagner relaxation is the expression of the dielectric loss. $\tan\delta$ tends to be zero in the Debye model when the frequency decreases to be zero, while reaches an infinite value in Maxwell-Wagner model, as depicted by equation (2) and (3), respectively.

$$\tan\delta = \frac{(\varepsilon_s - \varepsilon_\infty)\omega\tau}{\varepsilon_s + \varepsilon_\infty\omega^2\tau^2} \quad (2)$$

$$\tan\delta = \frac{(\varepsilon_s - \varepsilon_\infty)\omega\tau}{\varepsilon_s + \varepsilon_\infty\omega^2\tau^2} + \frac{\sigma}{\omega\varepsilon_0}\left(\frac{1}{\varepsilon_\infty + (\varepsilon_s - \varepsilon_\infty/1 + \omega^2\tau^2}\right) \quad (3)$$

where ε_s and ε_∞ are the static and optical-frequency dielectric constant, respectively, τ and ω are the relaxation time and angular frequency ($\omega=2\pi f$, and f is the frequency), respectively, ε_0 is the vacuum dielectric constant, and σ is the resistivity. As Figure 4(b) shows, $\tan\delta$ of all the specimens at low frequency range is beyond of zero due to their low resistivity, which in accordance with the results of equation (3). Therefore, Maxwell-Wagner relaxation becomes a dominant factor in the dielectric properties of ZnO ceramics at low frequencies, which is crucial in many non-ferroelectric high dielectric constant materials.[9]

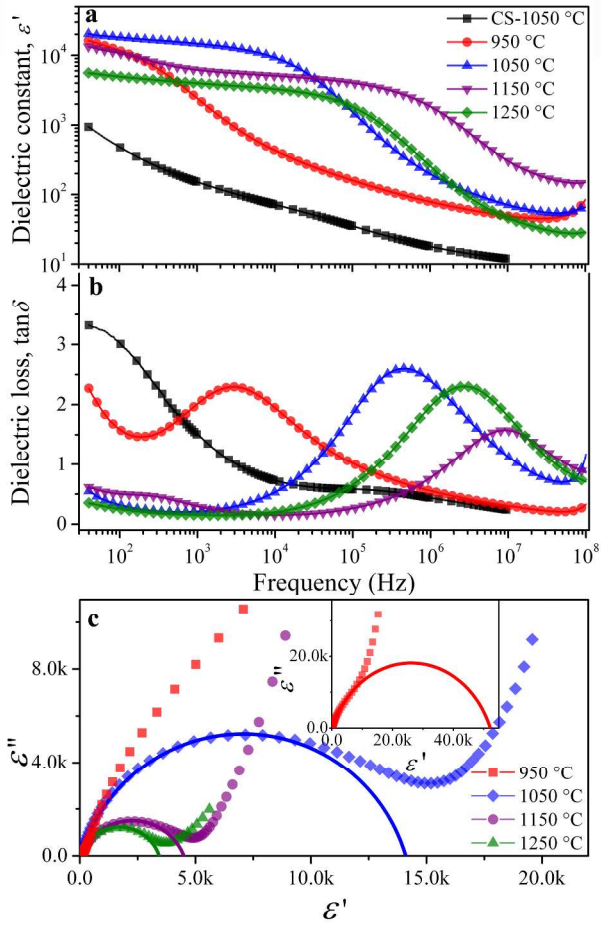

Figure 4 Frequency dependence of (a) ε', (b) tanδ, and (c) Cole-Cole plots of ZnO ceramics with HPT, the inset is the Cole-Cole plots of 950 °C sintered specimen.

The dielectric relaxation nature is usually investigated by complex Cole-Cole plots, as described by the following relationship.[19]

$$\varepsilon^* = \varepsilon' - j\varepsilon'' = \varepsilon_\infty + \frac{\varepsilon_s - \varepsilon_\infty}{1+(j\omega\tau)^{1-\alpha}} \quad (4)$$

where α is the distribution of relaxation time and the value of $\alpha\pi/2$ denotes the angle between the ε' axis and the line to the circle centre from the high-frequency intercept. Figure 4(c) displays Cole-Cole plots of ZnO ceramics with HPT sintered at 950°C, 1050 °C, 1150°C and 1250 °C. For ideal mono-dispersive relaxation α=0. The circle centers of all ZnO ceramics locate below the ε' axis, giving α value between 0.1 and 0.3, demonstrating that the dielectric relaxation nature of the porous ZnO ceramics is not an ideal mono-dispersive relaxation but a poly-dispersive relaxation. The semi-circle of specimen sintered at 950 °C has the largest diameter due to its high dielectric loss at low frequency as shown in the inset of Figure 4(c), while the large diameter of specimen sintered at 1050 °C is attributed to its giant dielectric constant.

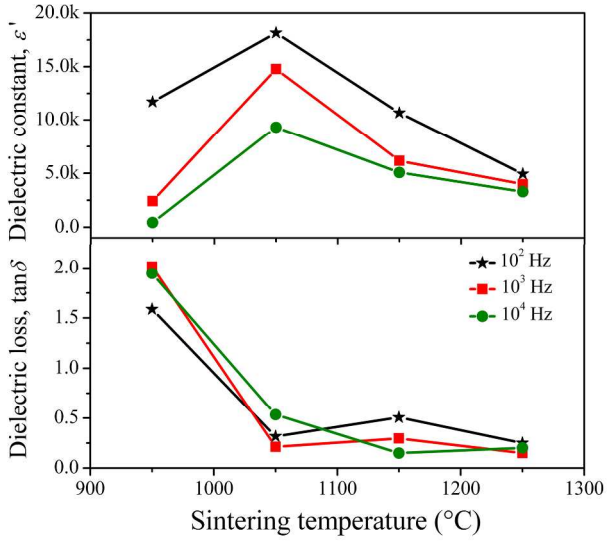

Figure 5 Variation of a) ε' and b) tanδ of HPT ZnO ceramics with sintering temperature at different frequencies.

Since space-charge polarization effect plays the dominant role when the relaxation frequencies f_p of the specimens lie in the range of around 10 Hz, the increase of ε' at frequencies below 100 Hz is primarily due to the space-charge polarization.[18c] In order to further investigate the variations of dielectric properties of HPT ZnO ceramics with sintering temperature, variation of ε' and tanδ with sintering temperature at 100, 1k, and 10k Hz are shown in Figure 5(a) and 5(b), respectively. As the relative density and grain size increase with increasing sintering temperature, it is obvious that ε' increases firstly and then decreases with the increase of relative density and grain size (Figure S4), while tanδ decreases with increasing relative density and grain size. It implies that both relative density and grain size play an important role in the dielectric properties of porous ZnO ceramics. Specimen sintered at 1050 °C presents the best dielectric properties with ε'=1.8×10^4, and tanδ=0.31 at 100 Hz due to its low grain boundary resistance and relaxation frequency caused by Maxwell-Wagner poly-dispersive relaxation as discussed above, especially, the obtained giant ε' is much higher than that of specimen without HPT and the reported ZnO ceramics,[14] and present good temperature stability as shown in Figure S5. In addition, specimen sintered at 1150 °C presents better high frequency stability, keeping a high value of 1861 at 1 MHz. Therefore, forming porous structure and low grain boundary resistance by high pressure treating introduce a new strategy and direction in improving the dielectric constant of ZnO ceramics, making them a new candidate giant dielectric constant material with low loss for industrial applications.

4. Conclusions

In summary, this work clearly demonstrates that the porous ZnO ceramics *via* high pressure treating show giant dielectric constant and low dielectric loss. The results described a remarkable dielectric performance arising from the porous structure and low density; the structure formed a low grain boundary resistance due to high pressure treating, which then led to enhanced Maxwell-Wagner poly-dispersive relaxation. These results suggest that high pressure treatment resulting in the formation of porous structure is an effective way for the

improvement of the dielectric properties of ZnO ceramics for the high dielectric constant applications.

Acknowledgements

The authors are thankful to Dr. D. Fan and F. Zhao for measurement of SEM, and thankful to Prof. W.J. Zhu at the Institute of Fluid Physics for helpful discussions. The authors are also thankful to the Foundation of National Key Laboratory of Shock Wave and Detonation Physics for financial support (Grant No. 9140C670302130C67239).

Notes and references

National Key Laboratory of Shock Wave and Detonation Physics, Institute of Fluid Physics, Chinese Academy of Engineering Physics, P.O. Box 919-111, Mianyang, 621900, People's Republic of China
E-mail: mcm901570@126.com (Chuanmin Meng), wangzg@caep.cn (Zhigang Wang); Tel/Fax: +86-816-2485105
Electronic Supplementary Information (ESI) available: See DOI: 10.1039/b000000x/

1 C.C. Homes, T. Vogt, S.M. Shapiro, S. Wakimoto, and A.P. Ramirez, *Science*, 2001, **293**, 673.
2 H. Han, C. Voisin, S.G. Fritsch, P. Dufour, C. Tenailleau, C. Turner, and J.C. Nino, *J. Appl. Phys*. 2013, **113**, 024102.
3 J.B. Wu, C.W. Nan, Y.H. Lin, and Y. Deng, *Phys. Rev. Lett.* 2002, **89**, 217601.
4 S. George, and M.T. Sebastian, *Compos. Sci. Technol.* 2008, **68**, 2461.
5 W.B. Hu, Y. Liu, R.L.Withers, T.J. Frankcombe, L. Norén, A. Snashall, M. Kitchin, P. Smith, B. Gong, H. Chen, J. Schiemer, F. Brink, and W.L. Jennifer, *Nat. Mater.* 2013, **12**, 821.
6 T.B. Adams, D.C. Sinclair, and A.R. West, *Adv. Mater.* 2002, **14** 1321; b) P. Lunkenheimer, S.Krohns, S.Riegg, S.G. Ebbinghaus, A. Reller, and A. Loidl, *Eur. Phys.-J. Spec. Top.* 2010, **180**, 61.
7 H. Zheng, W.J. Weng, G.R. Han, and P.Y. Du, *J. Phys. Chem. C* 2013, **117**, 12966.
8 a) M. Idrees, M. Nadeem, M. Atif, M. Siddique, M. Mehmood, and M.M. Hassan, *Acta Mater.* 2011, **59**, 1338; b) H. Wang, G.S. Li, M.L. Zhao, and L.P. Li, *Appl. Phys. Lett.* 2012, **100**, 152109.
9 a) P. Lunkenheimer, R. Fichtl, S. G. Ebbinghaus, and A. Loidl, *Phys. Rev. B*, 2004, **70**, 172102; b) L. Zhang, and Z.J. Tang, *Phys. Rev. B*, 2004, **70**, 174306; c) J.J. Liu, C.G. Duan, W.G. Yin, W.N. Mei, R.W. Smith, and J.R. Hardy, *Phys. Rev. B*, 2004, **70**, 144106.
10 a) J. Shi, M.B. Starr, and X.D. Wang, *Adv. Mater.* 2012, **24**, 4683-4691; b) Z.L. Wang, *Nano Today*, 2010, **5**, 540.
11 a) M.E. Abrishami, A. Kompany, and S.M. Hosseini, *J. Electroceram.* 2012, **29**, 125. b) J. Wu, T.T. Li, T. Qi, Q.W. Qin, G.Q. Li, B.L. Zhu, R. Wu, and C.S. Xie, *J. Electron. Mater.* 2012, **41**, 1970.
12 S.J. Shi, X.P. Zhuang, B.W. Cheng, and X.Q. Wang, *J. Mater. Chem. A*, 2013, **1**, 13779.
13 Y.Y. Qi, Z. Wang, M.L. Zhang, F.H. Yang, and X.D. Wang, *J. Mater. Chem. A*, 2013, **1**, 6110.
14 a) R. Tripathi, A. Kumar, C. Bharti, and T.P. Sinha, *Curr. Appl. Phys.* 2010, **10**, 676; b) M. Nadeem, AminaFarooq, and T. J. Shin, *Appl. Phys. Lett.* 2010, **96**, 212104; c)Y. Yang, W. Guo, X.Q. Wang, Z.Z. Wang, J.J. Qi, and Y. Zhang, *Nano Lett.* 2012, **12**, 1919; d) A.K. Giri, A. Sinhamahapatra, S. Prakash, J. Chaudhari, V.K. Shahi, and A.B. Panda, *J. Mater. Chem. A*, 2013, **1**, 814;e) G.S. Wang, Y.Y. Wu, X.J. Zhang, Y. Li, L. Guo, and M.S. Cao, *J. Mater. Chem. A*, 2014, **2**, 8644.
15 a) A. Soukiassian, A. Tagantsev, and N. Setter, *Appl. Phys. Lett.* 2010, **97**, 192903; b) V. Kapustianyk, Y. Eliyashevskyy, B. Turkoa, Z. Czapla, S. Dacko, and B. Barwinski, *J. Alloys Compd.* 2012, **531**, 64.
16 a) M.A. Seitz, and T.O. Sokoly, *J. Electrochem. Soc.* 1974, **121**, 163; b) A.K. Azad, J.G. Han, and W.L. Zhang, *Appl. Phys. Lett.* 2006, **88**, 021103.
17 a) D. Chandra, N. Mukherjee, A. Mondal, and A. Bhaumik, *J. Phys. Chem. C*, 2008, **112**, 8668; b) A.K. Yang, C.A. Wang, R. Guo, and Y. Huang, *Appl. Phys. Lett.* 2011, **98**, 152904; c) F. Brouersti, and A. Ramsamugh, *J. Phys. C: Solid State Phys.* 1988, **21**, 1839; d) F. Claro, and F. Brouers, *Phys. Rev. B* 1989, **40**, 3261; e) D. Piazza, C. Capiani, and G. Galassi, *J. Eur. Ceram. Soc.* 2005, **25**, 3075.
18 a) J. Jose, and M.A. Khadar, *Acta Mater.*2001, **49**, 729; b)R. Shao, S.V. Kalinin, and D.A. Bonnell, *Appl. Phys. Lett.* 2003, **82**, 1869; c) G.J. Wang, C.C. Wang, S.G. Huang, C.M. Lei, X.H. Sun, T. Li, and L.N. Liu, *J. Am. Ceram. Soc.* 2013, **96**, 2203; d) E. Barsoukov, and J.R. Macdonald, Impedance Spectroscopy Theory, Experiments, and Applications, Wiley Press, New York, 2nd ed., 2005.
19 a) Z.W. Yin, Dielectric Physics, Science Press, Beijing, 2nd ed., 2003; b) P. Lunkenheimer, V. Bobnar, A.V. Pronin, A.I. Ritus, A.A. Volkov, and A. Loidhl, *Phys. Rev. B*, 2002, **66**, 052105; c) A.K. Jonscher, Dielectric Relaxation in Solids, Chelsea Dielectric Press, London, 1983.
20 a) R.J. Wagner, *Ann. Phys.* 1913, **40**, 817; b) J.C. Maxwell, Treatise on Electricity and Magnetism, Dover, New York, 3rd ed., 1991.